

This discussion paper is/has been under review for the journal Hydrology and Earth System Sciences (HESS). Please refer to the corresponding final paper in HESS if available.

Groundwater flow processes and mixing in active volcanic systems: the case of Guadalajara (Mexico)

A. Hernández-Antonio¹, J. Mahlknecht¹, C. Tamez-Meléndez¹, J. Ramos-Leal²,
A. Ramírez-Orozco¹, R. Parra¹, N. Ornelas-Soto¹, and C. J. Eastoe³

¹Centro del Agua para América Latina y el Caribe, Tecnológico de Monterrey,
Monterrey, Mexico

²División de Geociencias Aplicadas, Instituto Potosino de Investigación Científica y
Tecnológica, San Luis Potosí, Mexico

³Department of Geosciences, University of Arizona, Tucson, USA

Received: 31 December 2014 – Accepted: 20 January 2015 – Published: 3 February 2015

Correspondence to: J. Mahlknecht (jurgen@itesm.mx)

Published by Copernicus Publications on behalf of the European Geosciences Union.

[Title Page](#)

[Abstract](#)

[Introduction](#)

[Conclusions](#)

[References](#)

[Tables](#)

[Figures](#)

[◀](#)

[▶](#)

[◀](#)

[▶](#)

[Back](#)

[Close](#)

[Full Screen / Esc](#)

[Printer-friendly Version](#)

[Interactive Discussion](#)

Abstract

Groundwater chemistry and **isotopic data** from 40 production wells in the Atemajac and Toluquilla Valleys, located in and around the Guadalajara metropolitan area, were determined to develop a conceptual model of groundwater flow processes and mixing.

5 Multivariate analysis including cluster analysis and principal component analysis were used to elucidate distribution patterns of constituents and factors controlling groundwater chemistry. Based on this analysis, groundwater was classified into four groups: cold groundwater, hydrothermal water, polluted groundwater and mixed groundwater. Cold groundwater is characterized by low temperature, salinity, and Cl and Na concentrations and is predominantly of Na-HCO₃ type. It originates as recharge at Primavera caldera and is found predominantly in wells in the upper Atemajac Valley. Hydrothermal water is characterized by high salinity, temperature, Cl, Na, HCO₃, and the presence of minor elements such as Li, Mn and F. It is a mixed HCO₃ type found in wells from Toluquilla Valley and represents regional flow circulation through basaltic and andesitic rocks. Polluted groundwater is characterized by elevated nitrate and sulfate concentrations and is usually derived from urban water cycling and subordinately from agricultural practices. Mixed groundwaters between cold and hydrothermal components are predominantly found in the lower Atemajac Valley. Tritium method elucidated that practically all of the sampled groundwater contains at least a small fraction of modern water. The multivariate mixing model M3 indicates that the proportion of hydrothermal fluids in sampled well water is between 13 (local groundwater) and 87 % (hydrothermal water), and the proportion of polluted water in wells ranges from 0 to 63 %. This study may help local water authorities to identify and quantify groundwater contamination and act accordingly.

1 Introduction

Active volcanic systems are frequently accompanied by an intense hydrothermal circulation, which is controlled by the exchange of mass and energy between groundwater systems, magmatic fluids and hot rock (Di Napoli et al., 2009; Goff and Janik, 2000).

5 The characterization of such hydrothermal systems helps on the one hand to quantify its geothermal energy potential and, on the other hand, to assess volcanic-related risks (Di Napoli et al., 2011). Hot springs, mud deposits, fumaroles, vaporization and degassing soils give initial clues about subsurface hydrothermal conditions (Hockstein and Browne, 2000; Navarro et al., 2011). The chemical characterization of fluids and
10 groundwater has been used as an indicator of the subsurface structure and the origin of released fluids when hydrogeological information is scarce (Appelo and Postma, 2005; Henley and Ellis, 1983). Hydrochemical data, such as high electrical conductivity (EC), high temperatures and elevated concentrations of As, B, Br, Cl, Cs, F, Fe, Ge, I, Li, Mn, Mo, Na, Rb, Sb, Ta, U and W denote the presence of hydrothermal fluids
15 in groundwater (Aksoy et al., 2009; Dogdu and Bayari, 2005; Reimann et al., 2003). However, hydrothermal volcanic systems are sometimes difficult to analyse due to the fact that groundwater is a mixture of fluids from various sources, sometimes consisting of shallow meteoric waters from recent infiltration, seawater and hydrothermal water rising from deep hydrothermal reservoirs (Chiodini et al., 2001; Di Napoli et al., 2009;
20 Evans et al., 2002).

The combination of different environmental tracer techniques helps elucidate the groundwater's origin, recharge, flow velocity and direction, residence or travel times, connections between aquifers, and surface and groundwater interrelations (Ako et al., 2013; Appelo and Postma, 2005; De Vries and Simmers, 2002; Edmunds and Smedley, 2000; Stumpf et al., 2014). These techniques have been applied in large semiarid to arid rift systems (Bretzler et al., 2011; Forrest et al., 2013; Furi et al., 2011; Ghiglieri et al., 2012; Panno et al., 2013; Siebert et al., 2012; Williams et al., 2013). Stable isotopes (^2H , ^{18}O) provide information regarding origins, recharge processes, flow paths

Groundwater flow processes and mixing in active volcanic systems

A. Hernández-Antonio et al.

[Title Page](#)

[Abstract](#)

[Introduction](#)

[Conclusions](#)

[References](#)

[Tables](#)

[Figures](#)

◀

▶

◀

▶

[Back](#)

[Close](#)

[Full Screen / Esc](#)

[Printer-friendly Version](#)

[Interactive Discussion](#)



and residence times, especially in fractured rock aquifers. Radioactive tracers like tritium (${}^3\text{H}$) are relatively inexpensive methods to estimate groundwater ages and characterize groundwater flow systems. Relatively few studies attempt to quantify mixing between different hydrothermal and cold fluids (Forrest et al., 2013).

5 This study was carried out in the Atemajac–Toluquilla aquifer system (ATAS) which underlies the metropolitan area of Guadalajara (~ 4.6 million inhabitants) and is located in a complex neotectonic active volcanic system in the Tepic–Zacoalco Rift. Adjacent to this aquifer system is the “La Primavera” caldera. Several survey wells have been drilled up to 3 km deep at La Primavera to explore the potential for geothermal energy (CFE, 2000). Temperatures between 80 and 300 °C have been registered in these wells (Verma et al., 2012), and temperatures higher than 40 °C have been measured in adjacent springs (Sánchez-Díaz, 2007). The hydrothermal fluids and springs are characterized by high concentrations of Na, Cl, SiO_2 , HCO_3 , B, F, and TDS. A mixture of hydrothermal fluids and meteoric-derived water has been identified in the springs of “La Primavera” (Sánchez-Díaz, 2007). While it is assumed that this caldera influences the aquifer system below the metropolitan area, the proportion of hydrothermal fluids and cold water is not clear. The diversity of the chemical results from previous studies has contributed to the difficulty in clearly evaluating the relationship between the fluids (see Results and Discussion section).

20 This study aims to understand the flow dynamics of groundwater by using the combination of statistical and geochemical methods. Water groups and factors that control the groundwater chemical processes were identified using a cluster and principal component analysis. Environmental tracers were used to assess chemical evolution. Mixing proportions of selected fluids in public wells were quantified by means of a multivariate 25 mixing calculation. This study is the first of its kind to report a comprehensive understanding of groundwater flow processes below the Guadalajara metropolitan area. This information is strategic to decision makers from local water authorities regarding water resources management.

[Title Page](#)[Abstract](#)[Introduction](#)[Conclusions](#)[References](#)[Tables](#)[Figures](#)[◀](#)[▶](#)[◀](#)[▶](#)[Back](#)[Close](#)[Full Screen / Esc](#)[Printer-friendly Version](#)[Interactive Discussion](#)

2 Study area

The study area is situated in the central portion of the state of Jalisco (Fig. 1). It belongs to the Lerma–Santiago river system, which drains into the Pacific Ocean. The climate in the study area is semi-warm to sub-humid. The National Water Commission reports an average annual temperature of 20.9 °C and an average annual precipitation of 904 mm, occurring mostly between May and October. The potential evaporation is on the order of 2000 mm (CONAGUA, 2010).

2.1 Hydrogeological settings

The study area is located in the western portion of the Mexican Volcanic Belt (MVB), a 1000 km-long volcanic arc that crosses central Mexico in E–W direction from the Pacific to the Atlantic Ocean. The MVB originated in the Late Miocene in response to the subduction of the Cocos and Rivera plates below the North American plate along the Middle America Trench. The belt has a composition of intermediate to silicic rocks (Alva-Valdivia et al., 2000). The western end of the MVB defines the fault-bounded crustal Jalisco Block (Ferrari et al., 2007; Valencia et al., 2013). The northern and eastern boundaries of this block consist of asymmetric continental rifts formed by tilted blocks with escarpments between 800 and 1000 m (Zárate-del Valle and Simoneit, 2005); the Tepic–Zacoalco Rift to the north runs in an NW–SE direction, and the Colima Rift to the east runs in an N–S direction; these rifts join the E–W oriented Citala or Chapala Rift in what is known as the Jalisco Triple Junction located 60 km SSW of the city of Guadalajara (Fig. 1). This area is a complex and active neotectonic structure that controls and regulates the development of the rift-floor, limited by normal faults (Michaud et al., 2000; Zárate-del Valle and Simoneit, 2005). The Atemajac and Toluquilla Valleys are located in the lower Tepic–Zacoalco Rift and are bordered by hills, volcanic cones (El Cuatro, San Martín), plateaus (Tonalá) and volcanic calderas (La Primavera), among other features (Sánchez-Díaz, 2007).

[Title Page](#)[Abstract](#)[Introduction](#)[Conclusions](#)[References](#)[Tables](#)[Figures](#)[◀](#)[▶](#)[◀](#)[▶](#)[Back](#)[Close](#)[Full Screen / Esc](#)[Printer-friendly Version](#)[Interactive Discussion](#)

These valleys consist of a relatively thin cover of Quaternary lacustrine deposits overlying a thick section of Neogene volcanic rocks including silicic domes, lava and cinder cones, lithic tuffs (Tala tuff), basalts, ignimbrites and other pyroclastic rocks, andesites and volcanic breccia, and a basement consisting of Oligocene granite

5 (Campos-Enríquez et al., 2005; Gutiérrez-Negrín, 1988; Urrutia et al., 2000). The principal aquifer, termed the Upper Aquifer unit, consists of the alluvium and underlying Neogene rocks. It is up to 700 m thick, and water is extracted from depths of up to 300 m below the surface (Sánchez-Díaz, 2007).

10 The water in the alluvial deposits and volcanic rocks in the upper aquifer unit is unconfined to semi-confined and moves under a natural hydraulic gradient that reflects the topography. In the Atemajac Valley, groundwater recharges in the normal fault NE from the La Primavera caldera from rainfall infiltration and flows in an SW-NE direction, while the flow in Toluquilla Valley starts in El Colli and moves in NW-SE direction (Figs. 1 and 2).

15 2.2 Hydrothermal system

The La Primavera caldera, with a diameter of ~10 km, borders the study area to the west. It is a very young (Late Pleistocene) volcanic complex underlain by a magma chamber whose top reaches a depth of 4 km (Verma et al., 2012). Drilling has revealed that the oldest units consist of granitic and granodioritic rocks found mainly at

20 a depth of approximately 3000 m. These rocks are mainly overlain by andesitic rocks approximately 1150 m thick. The third lithologic unit, which is approximately 100 m thick, consists of rhyolites. The uppermost unit is a sequence of lithic tuffs and minor andesite with an average thickness of approximately 750 and 1000 m, respectively (Campos-Enríquez et al., 2005; Urrutia et al., 2000; Verma et al., 2012). The system is characterized by an asymmetric structure with NW-SE regional basalt lineaments that belong to the Tepic Zacoalco Rift and local NE-SW fractures in the upper units extending beneath Guadalajara (Alatorre-Zamora and Campos-Enríquez, 1991; Campos-Enríquez and Alatorre-Zamora, 1998). The temperatures, which were

Title Page

Abstract

Introduction

Conclusions

References

Tables

Figures

◀

▶

◀

▶

Back

Close

Full Screen / Esc

Printer-friendly Version

Interactive Discussion

measured at the bottom of exploratory wells that were drilled up to 3 km deep, vary from 80 to 300 °C (Verma et al., 2012). It appears that heated meteoric water ascends along fault or fracture zones to near surface depths and supplies springs with temperatures of > 40 °C (Venegas et al., 1985). The hydrothermal fluids are characterized by very high concentrations of Na (679–810 mg L⁻¹), Cl (865–1100 mg L⁻¹), SiO₂ (943–1320 mg L⁻¹), B (75–150 mg L⁻¹) and TDS (2810–4065 mg L⁻¹) (Maciel-Flores and Rosas-Elguera, 1992), while the springs are of Na-Cl-HCO₃ type with relatively high concentrations of Na (260–331 mg L⁻¹), Cl (85–185 mg L⁻¹), SiO₂ (209–253 mg L⁻¹), HCO₃ (395–508 mg L⁻¹), B (10.8–12.3 mg L⁻¹), F (8.5 mg L⁻¹) and TDS (1071–1240 mg L⁻¹), indicating a mixture between hydrothermal fluids and local rain-water origin with ratios of 1 : 2 to 1 : 10 (Gutiérrez-Negrín, 1988; Sánchez-Díaz, 2007).

3 Methods

3.1 Field and laboratory

Water samples were collected from 40 production wells in March 2011 using standard protocols. The samples were analyzed for major and minor ions, trace elements and isotopes ($\delta^2\text{H}$, $\delta^{18}\text{O}$, ^3H). Field parameters such as temperature, pH, electrical conductivity (EC), and dissolved oxygen (DO), were measured using portable meters (Thermo, Orion). Alkalinity was determined in the field by volumetric titration (0.02 N H₂SO₄) of filtered water samples to pH 4.3. At each sampling site, new and pre-rinsed low density polyethylene bottles were filled with filtered (0.45 µm) sample water. Cation and silica samples were acidified with ultrapure HCl to pH < 2, and all of the samples were stored in the laboratory at a constant temperature of 4 °C. Dissolved cations and anions were determined by inductive-coupled plasma mass spectrometry (ICP-MS) and ion chromatography, respectively. Duplicates of selected samples were analyzed using inductive-coupled plasma optical emission spectrometry (ICP-OES) and ion chromatography, following standard methods (APHA, 2012).

[Title Page](#)

[Abstract](#)

[Introduction](#)

[Conclusions](#)

[References](#)

[Tables](#)

[Figures](#)

[◀](#)

[▶](#)

[◀](#)

[▶](#)

[Back](#)

[Close](#)

[Full Screen / Esc](#)

[Printer-friendly Version](#)

[Interactive Discussion](#)

Water isotopes were analyzed at EIL, University of Waterloo, Canada. To conduct deuterium (^2H) analyses, sample water was reduced on hot manganese (512°C) and the released hydrogen was analyzed by GC-MS. To conduct oxygen-18 (^{18}O) analyses, water was equilibrated with CO_2 . Preparation and extraction took place on a fully

5 automated system vessel attached to a VG MM 903 mass spectrometer. The ^2H and ^{18}O results are reported as δ -values with respect to the VSMOW (Vienna Standard Mean Ocean Water) standard. The samples were analyzed for tritium (^3H) by a liquid scintillation counter after electrolytic enrichment.

3.2 Interpretation

10 A preliminary description of water chemistry and identification of possible processes was performed using a correlation analysis. A hierarchical cluster analysis (HCA) organized samples into classified groups which were evaluated according to their geographic correspondence. A principal component analysis (PCA) elucidated the main controls on groundwater chemistry. All of the statistical calculations were performed
15 using Minitab version 17.1 (Minitab, 2013).

The multivariate mixing and mass balance model, or M3 (Laaksoharju et al., 2008), was used to help to understand groundwater composition. The main aim of M3 is to differentiate between what is due to mixing and what is due to water-rock reactions. The M3 method compares the measured groundwater composition of each sample to
20 the selected reference water and reports the changes in terms of mixing and reactions. A PCA is used to summarize the groundwater data by using the majority of the dissolved groundwater constituents Ca , Na , Mg , K , Cl , SO_4 and HCO_3 in combination with the isotopes $\delta^2\text{H}$, $\delta^{18}\text{O}$ and ^3H . The outcome of the analyses can be visualized as a scatter plot (PCA plot) for the first two principal components. The observations inside the polygon of the PCA plot are compared to the previously chosen reference water compositions. The mixing calculations create ideal mixing models that use linear distances of the samples from the selected reference waters in the PCA plot. In this
25

[Title Page](#)

[Abstract](#)

[Introduction](#)

[Conclusions](#)

[References](#)

[Tables](#)

[Figures](#)

◀

▶

[Back](#)

[Close](#)

[Full Screen / Esc](#)

[Printer-friendly Version](#)

[Interactive Discussion](#)

study, the following sample compositions were used as reference waters: AT5 – highest temperature and salinity as the reference for hydrothermal fluids; AT12 – low temperature and elevated salinity as the reference for polluted or anthropogenically impacted water; and AT37 – low temperature and salinity as the reference for local groundwater.

5 Although none of these selected reference waters are considered end members, they were selected as most representative for the purpose of the present study to determine the amounts of each mixture.

4 Results and discussion

Sánchez-Díaz (2007) used groundwater temperature and total dissolved solids as criteria to classify wells in hydrothermal water from Toluquilla (HT), hydrothermal water from

10 springs NE of Guadalajara (HG), non-hydrothermal, local groundwater (LG), and mixed groundwater (MG) with both HT and LG (Fig. 3). Considering different sets of historical and new data, this classification is too subjective, especially in the lower TDS range. Furthermore, some inconsistencies between correlation results from different sampling

15 campaigns show that the interpretation is not straightforward. The Mg concentration, for example, decreases with increasing temperature as expected from hydrothermal fluids (Panichi and Gonfiantini, 1981); on the other hand, an increasing Mg trend at low temperatures is observed indicating saline groundwater. Finally, it was not clear if there are different sources of hydrothermal or saline waters that affect the local groundwater.

20 These complications motivated us to use multivariate techniques instead of commonly used scatterplots and criteria to divide samples into groups and interpret for potential factors/sources. Because the measured parameters varied considerably from study to study, only data from this study were considered for the multivariate techniques.

[Title Page](#)

[Abstract](#)

[Introduction](#)

[Conclusions](#)

[References](#)

[Tables](#)

[Figures](#)

◀

▶

◀

▶

[Back](#)

[Close](#)

[Full Screen / Esc](#)

[Printer-friendly Version](#)

[Interactive Discussion](#)

4.1 Multivariate statistics

Table 1 shows the concentrations of measured groundwater elements, field parameters and isotopic ratios, along with the hydrochemical classification.

The classification of waters was performed with HCA using 20 variables (pH, temperature, EC, DO, Na, K, Ca, Mg, Cl, HCO_3 , SO_4 , NO_3 -N, Sr, SiO_2 , Fe, F, Zn, ${}^3\text{H}$, ${}^2\text{H}$, ${}^{18}\text{O}$). With the help of Ward's linkage rule iteratively neighboring points (samples) were linked through a similarity matrix (Ward, 1963). The squared Euclidian distance was selected as the similarity measurement. The second method was a PCA. For both cluster algorithms, lognormal distributed data were previously log-transformed, and all of the variables standardized (z-scores). The HCA samples were classified into 4 major groups as represented by the dendrogram in Fig. 4 and median values (Table 2). The values for Li, Mn and Ba were not considered in the cluster analysis, because most samples had concentrations below the detection limit.

Group 1 ($n = 6$) had the highest temperatures (average 33.8°C), high salinity (EC = $1575 \mu\text{Scm}^{-1}$), and low NO_3 -N (0.17 mg L^{-1}) and ${}^3\text{H}$ (0.73 TU) values, along with traces of Li, Mn and Ba that were possibly due to geothermal influence. These waters were of mixed HCO_3 type, as shown in the Piper diagram (Fig. 5), and located in the central area of Toluquilla. Group 2 ($n = 12$) had slightly lower temperatures (30.2°C), with considerably lower salinity ($300 \mu\text{Scm}^{-1}$) and ${}^3\text{H}$ activity similar to that of group 1. Chloride concentrations are low (3.5 mg L^{-1}) compared to the other groups. Wells from group 2 were found mainly in the eastern and southern region of the study area. These waters were of Na- HCO_3 to mixed HCO_3 type. The smallest group 3 ($n = 3$) represents the coldest waters (23.4°C), that had variable salinity (EC = $556 \mu\text{Scm}^{-1}$), and the highest SO_4 (70.6 mg L^{-1}), NO_3 -N (12.4 mg L^{-1}), ${}^3\text{H}$ (2.1 TU) values, and relatively elevated Na (52.2 mg L^{-1}) and Cl (38.9 mg L^{-1}) concentrations. These waters were a mixture of Na- SO_4 to mixed HCO_3 type, located in urban and agricultural areas, possibly indicating anthropogenic pollution. Finally, group 4 ($n = 19$) was cold (25.3°C), similar to group 3, with low salinity ($254 \mu\text{Scm}^{-1}$), and elevated NO_3 -N (9.1 mg L^{-1}) and SO_4

[Title Page](#)

[Abstract](#)

[Introduction](#)

[Conclusions](#)

[References](#)

[Tables](#)

[Figures](#)

◀

▶

◀

▶

[Back](#)

[Close](#)

[Full Screen / Esc](#)

[Printer-friendly Version](#)

[Interactive Discussion](#)

(15.5 mg L⁻¹) values. These predominantly Na-HCO₃ to mixed HCO₃ type waters are located in the western portion of the aquifer system in areas of elevated altitude where most of the recharge takes place. Figure 5 shows that groups 3 and 4 are relatively similar compared to the other two groups.

5 A factor analysis transformed the 20 variables into a reduced number of factors. The PCA, which loads most of the total variance onto one factor, was used in this study. The factors were extracted through the principal components method. Varimax rotation, where one factor explains mostly one variable, was selected. For fixing the maximum number of factors to be extracted, only factors with eigenvalues higher than 10 one were taken into consideration (Kaiser normalization).

Table 3 shows that 4 factors may explain 77 % of the variance. Factor 1 (42 % of the variance) largely represents high salinity. The correlations of temperature, Na and Cl indicate hydrothermal influence, while HCO₃, Na and Sr could be connected to mineralization and rock dissolution processes, and cationic exchange. In factor 2 (17 %) the 15 temperature is inversely related with DO, ³H, and to a lesser degree, NO₃ and SO₄, suggesting that this factor represents water affected by human activities, either urban or agricultural. In addition, Table 1 shows that waters affected by human activities are most evaporated. Sulfate could be related to contamination due to the infiltration of 20 commonly applied sulfate-based fertilizers during the rainy season. This occurs because all the wells are undersaturated with regard to gypsum, indicating that the water does not move through deposits of this mineral. In factor 3 (11 %) the relationship between ²H and ¹⁸O reveals the existence of recharge water. This factor is generated almost entirely by the linear relationship between O and H isotopes. The relation with 25 temperature indicates the recharge conditions at different recharge sites. Factor 4 (7 %) may be indicative of dissolution of minerals that contain F. The study of Sánchez-Díaz (2007) indicates that the rhyolitic rocks and ashes of the study area are responsible for releasing F. Comparable trends have been observed in similar volcanic environments in central and northern Mexico (Mahlknecht et al., 2004, 2008).

[Title Page](#)[Abstract](#)[Introduction](#)[Conclusions](#)[References](#)[Tables](#)[Figures](#)[◀](#)[▶](#)[◀](#)[▶](#)[Back](#)[Close](#)[Full Screen / Esc](#)[Printer-friendly Version](#)[Interactive Discussion](#)

4.2 Isotope hydrology

The $\delta^2\text{H}$ vs. $\delta^{18}\text{O}$ graph shows that the analyzed groundwater is of meteoric origin with variable evaporation and hydrothermal effects (Fig. 6a and b). Group 1 (hydrothermal influenced) waters, collected in Toluquilla, have a narrow range of $\delta^{18}\text{O}$ (−9.4 to −8.8‰) and $\delta^2\text{H}$ (−67 to −68‰) values. They tend to fall slightly below and parallel to the RMWL, possibly indicating different climate conditions during recharge. The increased Cl concentrations compared to other groups evidences mixture with hydrothermal fluids (Fig. 6b). Group 2 waters, collected in the eastern and southern part of the ATAS, have $\delta^{18}\text{O}$ values ranging from −9.6 to −8.6‰, and $\delta^2\text{H}$ values from −63 to −71‰. These waters fall along the regional meteoric water line. Group 3 waters (influenced by anthropogenic pollution) are quite different from the rest; they have $\delta^{18}\text{O}$ values ranging from −7.9 to −5.7‰, and $\delta^2\text{H}$ values from −59.6 to −47.5‰, and are strongly affected by evaporation (Fig. 6b). The enriched outlier AT12 represents groundwater from a recreational park with lagoons. Group 4 waters, mostly from La Primavera recharge area, are covering a relative wide range of values compared to group 1 and 2. Their $\delta^{18}\text{O}$ signatures vary from −10.3 to −8.4‰, and their $\delta^2\text{H}$ signatures from −72.2 to −63.9‰. The overlapping of group 1, 2 and 4 indicates that aquifer formations are mostly hydraulically interconnected. Although altitude variations are in the order of only 400 m around La Primavera Caldera, this seems to be enough to generate an altitude effect (Fig. 6c).

Tritium results indicate that groundwater within the study area includes both pre-modern (pre-1950s) and modern recharge. The values range from 0.3 to 3.0 TU which indicates a contribution from modern water in every sampled site (Table 1). The majority of waters with ^3H lower than 1.0 TU are in the southern portion of the aquifer system.

25 4.3 Mixing patterns with M3

The M3 mixing model compared all the samples to the three reference-water components (hydrothermal water – HW, groundwater – GW, human impacted water – HIW).

[Title Page](#)

[Abstract](#)

[Introduction](#)

[Conclusions](#)

[References](#)

[Tables](#)

[Figures](#)

◀

▶

◀

▶

[Back](#)

[Close](#)

[Full Screen / Esc](#)

[Printer-friendly Version](#)

[Interactive Discussion](#)

The calculation results indicate that the proportion of hydrothermal fluids within group 1 wells is between 32 and 87 % (Fig. 7, Table 4), while the proportion is lower than 13 % within the other three groups. On the other hand, anthropogenically impacted waters within group 3 show proportions between 59 and 63 %, while all of the other groups 5 are lower than 36 %. These results validate the initial selection of groups based on cluster analysis. Geographically, groundwater with elevated hydrothermal proportions is located in the south to southeastern area (Toluquilla), and elevated proportions of polluted groundwater are located mostly in the urbanized area of Guadalajara. Samples AT7, AT11, AT29, AT35 and AT38 lie outside the polygon in Fig. 7 and have thus 10 been excluded from evaluation. However, note that they represent local groundwaters and indicate that the selected reference waters are only an approximation of unknown 15 end members, so the polygon may not include all of the samples.

4.4 Groundwater flow system of Guadalajara

The hydrogeological Atemajac–Toluquilla system is located in the northeastern area 15 of the Tepic–Zacoalco Rift, a complex and active neotectonic structure. Local ground- water recharge for Atemajac–Toluquilla Valley originates from rainfall mainly over the La Primavera caldera in the central western portion of the study unit. It flows in the 20 upper alluvial sediments towards the valley floor and Santiago River. It is characterized by low temperature, and SDT, Cl and Na concentrations, and is of predominantly Na-HCO₃ type. This kind of groundwater predominates in the western Atemajac Valley.

Underground heat flow suggests the existence of a magma chamber below the La Primavera caldera, which provides hydrothermal fluids observed on surface expressions such as the La Soledad solfatara and the Cerritos Colorados geothermal field. These emerging fluids circulate towards the deeper Atemajac–Toluquilla aquifer 25 unit specifically below Santa Anita and Toluquilla. Calcedonia geothermometers indicate that these fluids are related to basaltic and andesitic rocks (San Cristobal group) (Sánchez-Díaz, 2007). They are characterized by elevated temperatures, salinity, Cl, Na and HCO₃ values, and contain Li, Mn, B and F, which indicate thermal influence, cir-

[Title Page](#)[Abstract](#)[Introduction](#)[Conclusions](#)[References](#)[Tables](#)[Figures](#)[◀](#)[▶](#)[◀](#)[▶](#)[Back](#)[Close](#)[Full Screen / Esc](#)[Printer-friendly Version](#)[Interactive Discussion](#)

culation through fault zones and an active volcanic center, and water-rock interactions. These waters are of mixed HCO_3 type. They are representative of the southwestern portion (Toluquilla Valley).

5 Polluted waters infiltrate mainly from urban water cycling and, to a minor degree, from agricultural plots. These waters are characterized by low temperature, variable salinity, high concentrations of nitrate and sulfate and, elevated concentrations of chloride and sodium, and are of Na-SO_4 to mixed HCO_3 type.

10 The isotopic composition of groundwater indicates interconnectivity between water from deeper and shallow rock materials. Practically all groundwater sampled contains at least a small fraction of modern water. The proportions of hydrothermal fluids in sampled well waters ranged from 13 (cold groundwater) to 87% (hydrothermal water), while the proportion of polluted water is between 0 and 63%. Figure 8 shows two schematic flow sections of Atemajac and Toluquilla valley.

5 Conclusions

15 This work represents the first time that groundwater flow dynamics of Guadalajara region have been analyzed and characterized by using a suite of statistical and geochemical methods. Geochemical methods have been combined with multivariate statistical analysis and the multivariate mixing and mass-balance model (M3) to determine the mixing patterns of different fluids when considering fresh groundwater, hydrothermal fluids and human impacted waters.

20 The initial classification of groundwater groups by cluster analysis has been confirmed by water isotopic technologies, and identifying the controlling factors by principle component analysis is consistent with M3 modeling. The origin of groundwater recharge and the mixture of fresh groundwater with hydrothermal fluids and polluted water components was identified. A conceptual flow model was constructed for the Atemajac–Toluquilla aquifer system. The local flow is associated with the infiltration of rainwater that occurs at higher altitudes. Hydrothermal waters are probably related to

recharge outside the study area and upward vertical flow in the La Primavera caldera and the valley of Toluquilla. TDS, Cl, Na, Mn and Li, are most indicative of hydrothermal fluids. Modern water polluted with SO_4 and NO_3 can be associated with urban development and agricultural practices. The proportion of hydrothermal fluids within older waters is between 32 and 87 %, whereas it is lower than 13 % within other waters.

These outcomes may help water authorities to identify wells with hydrothermal mixture or polluted water and act accordingly. The information regarding the proportions of fresh groundwater, hydrothermal fluids and polluted waters in each well indicates that the contaminants can be attributed to source waters. For example, Li, Mn, Ba, F and

As can be associated with hydrothermal fluids, and SO_4 and NO_3 are related to the production or use of fertilizers, dyes, glass, paper, soaps, textiles, fungicides or insecticides. This result helps authorities to decide whether certain wells have to be isolated or closed in order to provide Guadalajara with the required drinking water quality.

M3 is a powerful tool to evaluate the mixing proportions of selected reference waters present in aquifers. We recommend the use of the suite of traditional methods, environmental tracers, statistical analysis and M3 modeling in other aquifers with potentially multiple groundwater origins, especially in active volcanic systems.

Acknowledgements. The authors thank Fundación FEMSA and the Chair for Sustainable Water Use (Tecnológico de Monterrey) for the financial support given to develop this investigation.

References

Ako, A. A., Eyong, G. E. T., Shimada, J., Koike, K., Hosono, T., Ichiyangai, K., Akoachere, R., Tandia, B. K., Nkeng, G. E., and Ntankouo, N. R.: Nitrate contamination of groundwater in two areas of the Cameroon Volcanic Line (Banana Plain and Mount Cameroon area), *Appl. Water Sci.*, 4, 99–113, 2013.

Aksay, N., Simsek, C., and Gunduz, O.: Groundwater contamination mechanism in a geothermal field: a case study of Balcova, Turkey, *J. Contam. Hydrol.*, 103, 13–28, 2009.

Alatorre-Zamora, M. A. and Campos-Enríquez J. O.: La Primavera Caldera (Mexico): structure inferred from gravity and hydrogeological considerations, *Geofis. Int.*, 31, 371–382, 1991.

Groundwater flow processes and mixing in active volcanic systems

A. Hernández-Antonio et al.

[Title Page](#)

[Abstract](#)

[Introduction](#)

[Conclusions](#)

[References](#)

[Tables](#)

[Figures](#)

[◀](#)

[▶](#)

[◀](#)

[▶](#)

[Back](#)

[Close](#)

[Full Screen / Esc](#)

[Printer-friendly Version](#)

[Interactive Discussion](#)

Alva-Valdivia, R., Goguitchaichvili, A., Ferrari, L., Rosas-Helguera, J., Urrutia-Fucugauchi, J., and Zambrano-Orozco, J. J.: Paleomagnetic data from the Trans-Mexican Volcanic Belt: implications for tectonics and volcanic stratigraphy, *Earth Planets Space*, 52, 467–478, 2000.

APHA: Standard Methods for examination of water and wastewater, 22nd Edn., American Public Health Association, Washington, 2012.

Appelo, C. A. J. and Postma, D.: *Geochemistry, Groundwater and Pollution*, 2nd Edn., A. A. Balkema, Leiden, The Netherlands, p. 649, 2005.

Bretzler, A., Osenbrück, K., Gloaguen, R., Ruprecht, J. S., Kebede, S., and Stadler, S.: Groundwater origin and flow dynamics in active rift systems – a multi-isotope approach in the Main Ethiopian Rift, *J. Hydrol.*, 402, 274–289, 2011.

Campos-Enríquez, J. O. and Alatorre-Zamora, M. A.: Shallow crustal structure of the junction of the grabens of Chapala, Tepic–Zacoalco and Colima, Mexico, *Geofis. Int.*, 37, 263–282, 1998.

Campos-Enríquez, J. O., Domínguez-Méndez, F., Lozada-Zumaets, M., Morales-Rodríguez, H. F., and Andaverde-Arredondo, J. A.: Application of the Gauss theorem to the study of silicic calderas: the calders of La Primavera, Los Azufres, and Los Humeros (Mexico), *J. Volcanol. Geoth. Res.*, 147, 39–67, 2005.

Chiodini, G., Marini, L., and Russo, M.: Geochemical evidence for the existence of high temperature hydrothermal brines at Vesuvio volcano, Italy, *Geochim. Cosmochim. Acta*, 65, 2129–2147, 2001.

CFE – Comisión Federal de Electricidad: Geotermia, Gerencia de Geotermia, Geotermia, Morelia, 23 pp., 2000.

CONAGUA – Comisión Nacional del Agua: Determinación de la Disponibilidad de Agua en el Acuífero Atemajac–Toluquilla), Estado de Jalisco (Determination of Water Availability in the Atemajac–Toluquilla aquifer, Jalisco state), México, D. F., 2010.

De Vries, J. J. and Simmers, I.: Groundwater recharge: an overview of processes and challenges, *Hydrogeol. J.*, 10, 5–17, 2002.

Di Napoli, R., Aiuppa, A., Bellomo, S., Brusca, L., D'Alessandro, W., Gagliano Candela, E., Longo, M., Pecoriano, G., and Valenza, M.: A model for Ischia hydrothermal system: evidences from the chemistry of thermal groundwaters, *J. Volcanol. Geoth. Res.*, 186, 133–159, 2009.

Di Napoli, R., Martorana, R., Orsi, G., Aiuppa, A., Camarda, M., De Gregorio, S., Gagliano Candela, E., Luzio, D., Messina, N., Pecoraino, G., Bitetto, M., de Vita, S., and Valenza, M.:

Groundwater flow processes and mixing in active volcanic systems

A. Hernández-Antonio et al.

[Title Page](#)

[Abstract](#)

[Introduction](#)

[Conclusions](#)

[References](#)

[Tables](#)

[Figures](#)

[◀](#)

[▶](#)

[◀](#)

[▶](#)

[Back](#)

[Close](#)

[Full Screen / Esc](#)

[Printer-friendly Version](#)

[Interactive Discussion](#)

The structure of a hydrothermal system from an integrated geochemical, geophysical and geology approach: the Ischia Island case study, *Geochem. Geophy. Geosy.*, 12, 1–25, 2011.

Dogdu, M. S. and Bayari, C. S.: Environmental impact of geothermal fluids on surface water, groundwater and streambed sediments in the Akarcay Basin, Turkey, *Environ. Geol.*, 47, 325–340, 2005.

Edmunds, W. and Smedley, P.: Residence time indicators in groundwater: the East Midlands Triassic sandstone aquifer, *Appl. Geochem.*, 15, 737–752, 2000.

Evans, W. C., Sorey, M. L., Cook, A. C., Kennedy, B. M., Shuster, D. L., Colvard, E. M., White, L. D., and Huebner, M. A.: Tracing and quantifying magmatic carbon discharge in cold groundwaters: lessons learned from Mammoth Mountain, USA, *J. Volcanol. Geoth. Res.*, 114, 291–312, 2002.

Ferrari, L., Valencia-Moreno, M., and Bryan, S.: Magmatism and tectonics of the Sierra Madre Occidental and its relation with the evolution of the western margin of North America, in: *Geology of México: Celebrating the Centenary of the Geological Society of México*, Special Paper 422, edited by: Alaniz-Álvarez, S. A. and Nieto-Samaniego, A. F., Geol. Soc. Am., Boulder, CO, 1–39, 2007.

Forrest, M. J., Kulogoski, J. T., Edwards, M. S., Farrar, C. D., Belitz, K., and Norris, R. D.: Hydrothermal contamination of public supply wells in Napa and Sonoma Valleys, California, *Appl. Geochem.*, 33, 25–40, 2013.

Furi, W., Razack, M., Abiye, T. A., Kebede, S., and Legesse, D.: Hydrochemical characterization of complex volcanic aquifers in a continental rifted zone: the Middle Awash Basin, Ethiopia, *Hydrogeol. J.*, 20, 385–400, 2011.

Ghiglieri, G., Pittalis, D., Cerri, G., and Oggiano, G.: Hydrogeology and hydrogeochemistry of an alkaline volcanic area: the NE Mt. Meru slope (East African Rift – Northern Tanzania), *Hydrol. Earth Syst. Sci.*, 16, 529–541, doi:10.5194/hess-16-529-2012, 2012.

Goff, F. and Janik, C. J.: Geothermal systems, in: *Encyclopedia of Volcanoes*, edited by: Sigurdsson, H., Houghton, B., McNutt, S., Rymer, H., and Stix, J., Academic Press, San Diego, CA, 817–834, 2000.

Gutiérrez-Negrín, L.: La Primavera, Jalisco, Mexico: geothermal field, *Transact. Geoth. Res. Council*, 12, 161–165, 1988.

Henley, R. W. and Ellis, A. J.: Geothermal systems, ancient and modern: a geochemical review, *Earth Sci. Rev.*, 19, 1–50, 1983.

Groundwater flow processes and mixing in active volcanic systems

A. Hernández-Antonio et al.

[Title Page](#)

[Abstract](#)

[Introduction](#)

[Conclusions](#)

[References](#)

[Tables](#)

[Figures](#)

[◀](#)

[▶](#)

[◀](#)

[▶](#)

[Back](#)

[Close](#)

[Full Screen / Esc](#)

[Printer-friendly Version](#)

[Interactive Discussion](#)

Hockstein, M. P. and Browne, P. R. L.: Surface manifestations of geothermal systems with volcanic heat sources, in: *Encyclopedia of Volcanoes*, edited by: Sigurdsson, H., Houghton, B., McNutt, S., Rymer, H., and Stix, J., Academic Press, San Diego, CA, 835–856, 2000.

Laaksoharju, M., Smellie, J., Tullborg, E- L., Gimeno, M., Molinero, J., Gurban, I., and Hallbeck, L.: Hydrogeochemical evaluation and modelling performed within the site investigation programme, *Appl. Geochem.*, 23, 1761–1795, 2008.

Maciel-Flores, R. and Rosas-Elguera, J.: *Modelo geológico y evaluación del campo geotérmico La Primavera*, Jal., México, *Geofis. Int.*, 31, 359–370, 1992.

Mahlknecht, J., Steinich, B., and Navarro de León, I.: Groundwater chemistry and mass transfers in the Independence aquifer, central Mexico, by using multivariate statistics and mass-balance models, *Environ. Geol.*, 45, 781–95, 2004.

Mahlknecht, J., Horst, A., Hernández-Limón, G., and Aravena, R.: Groundwater geochemistry of the Chihuahua City region in the Rio Conchos Basin (northern Mexico) and implications for water resources management, *Hydrol. Process.*, 22, 4736–4751, 2008.

Michaud, F., Gasse, F., Bourgois, J., and Quintero, O.: Tectonic controls on lake distribution in the Jalisco Block area (western Mexico) from Pliocene to Present, in: *Cenozoic Tectonics and Volcanism of Mexico*, Special paper 334, edited by: Delgado-Granados, H., Aguirre-Díaz, G. J., and Stock, J. M., *Geol. Soc. Am.*, Boulder, CO, 99–110, 2000.

Minitab: Statistical Software (versión 17.1). MINITAB® and all other trademarks and logos for the Company's products and services are the exclusive property of Minitab Inc. All other marks referenced remain the property of their respective owners, 2013.

Navarro, A., Font, X., and Viladevall, M.: Geochemistry and groundwater contamination in the La Selva geothermal system (Girona, Northeast Spain), *Geothermics*, 40, 275–285, 2011.

Panichi, C. and Gonfiantini, R.: Geothermal waters, in: *Stable Isotope Hydrology*, edited by: Gat, J. R. and Gonfiantini, R., IAEA Tech. Rep. Ser., IAEA, Vienna, 241–272, 1981.

Panno, S. V., Hackley, K. C., Locke, R. A., Krapac, I. G., Wimmer, B., Iranmanesh, A., and Kelly, W. R.: Formation waters from Cambrian-age strata, Illinois Basin, USA: constraints on their origin and evolution based on halide composition, *Geochim. Cosmochim. Acta*, 122, 184–197, 2013.

Reimann, C., Bjorvatn, K., Frengstad, B., Melaku, Z., Tekle-Haimanot, R., and Siewers, U.: Drinking water quality in the Ethiopian section of the East African Rift Valley I – data and health aspects, *Sci. Total. Environ.*, 311, 65–80, 2003.

Groundwater flow
processes and
mixing in active
volcanic systems

A. Hernández-Antonio et
al.

[Title Page](#)

[Abstract](#)

[Introduction](#)

[Conclusions](#)

[References](#)

[Tables](#)

[Figures](#)

[◀](#)

[▶](#)

[◀](#)

[▶](#)

[Back](#)

[Close](#)

[Full Screen / Esc](#)

[Printer-friendly Version](#)

[Interactive Discussion](#)

Sánchez-Díaz, L. F.: Origen, transporte, distribución y concentraciones de los fluoruros en el sistema hidrogeológico volcánico Atemajac–Toluquilla, Jalisco, México, PhD thesis, Universidad Nacional Autónoma de México, México, 128 pp., 2007.

Siebert, C., Rosenthal, E., Möller, P., Rödiger, T., and Meiler, M.: The hydrochemical identification of groundwater flowing to the Bet She'an–Harod multiaquifer system (Lower Jordan Valley) by rare earth elements, yttrium, stable isotopes (H, O) and Tritium, *Appl. Geochem.*, 27, 703–714, 2012.

Stumpf, C., Ekdal, A., Gönenc, I. E., and Maluszewski, P.: Hydrological dynamics of water sources in a Mediterranean lagoon, *Hydrol. Earth Syst. Sci.*, 18, 4825–4837, doi:10.5194/hess-18-4825-2014, 2014.

Urrutia, F. J., Alva-Valdivia, L. M., Rosas-Elguera, J., Campos-Enriquez, O., Goguitchaichvili, A., Soler-Arechalde, A. M., Caballero-Miranda, C., Venegas-Salgado, S., and Sanchez-Reyes, S.: Magnetostratigraphy of the volcanic sequence of Río Grande de Santiago-Sierra de la Primavera region, Jalisco, western Mexico, *Geofis. Int.*, 39, 247–265, 2000.

Valencia, V. A., Righter, K., Rosas-Elguera, J., Lopez-Martinez, M., and Grove, M.: The age and composition of the pre-Cenozoic basement of the Jalisco Block: implications for and relation to the Guerrero composite terrane, *Contrib. Mineral. Petr.*, 166, 801–824, 2013.

Venegas, S., Herrera, J. J., and Maciel, F. R.: Algunas características de la Faja Volcánica Mexicana y de sus recursos geotérmicos, *Geofis. Int.*, 24, 47–83, 1985.

Verma, S. P., Arredondo-Parra, U. C., Andaverde, J., Gómez-Arias, E., and Guerrero-Martínez, F. J.: Three-dimensional temperature field simulation of a cooling of a magma chamber, La Primavera caldera, Jalisco, Mexico, *Int. Geol. Rev.*, 54, 833–843, 2012.

Ward, J. H.: Hierarchical grouping to optimize an objective function, *J. Am. Stat. Assoc.*, 58, 236–244, 1963.

Williams, A. J., Crossey, L. J., Karlstrom, K. E., Newell, D., Person, M., and Woolsey, E.: Hydrogeochemistry of the Middle Rio Grande aquifer system – fluid mixing and salinization of the Rio Grande due to fault inputs, *Chem. Geol.*, 351, 281–298, 2013.

Zarate-del Valle, P. F. and Simoneit, B. R. T.: La generación de petróleo hidrotermal en sedimentos del Lago Chapala y su relación con la actividad geotérmica del rift Citala en el estado de Jalisco, *Rev. Mex. Cienc. Geol.*, 22, 358–370, 2005.

Groundwater flow processes and mixing in active volcanic systems

A. Hernández-Antonio et
al.

Title Page

Abstract

Introduction

Conclusion

References

Tables

Figures

1

1

Back

Close

Full Screen / Esc

Interactive Discussion

ID	Well name	Well depth (m)	pH	T (°C)	EC (uS·cm⁻¹)	DO	Na	K	Ca	Mg	Cl	HCO₃	SO₄	NO₃-N	Sr	SiO₂	Fe
AT1	Toliquilla 1	300	7.3	25	345	5.34	44.2	6.8	13.3	4.9	9.4	146.4	21.5	3.8	0.07	44	0.05
AT2	Toliquilla 6	300	7.0	25	1619	5.76	152.0	58	28.9	103	70.1	1068.6	6.5	< 0.04	0.38	38.5	0.14
AT3	Toliquilla 17	200	7.0	25	2310	5.25	114.0	36	58.7	92.9	82.4	1031.3	5.0	0.07	0.45	35.1	0.18
AT4	Toliquilla 22	300	7.0	31.8	1792	5.1	147.0	40.9	89.7	113	85.4	1415.2	6.6	< 0.04	0.61	53.6	0.05
AT5	Toliquilla 7	230	7.0	36.4	1900	5.48	174.0	48.4	80.7	104	229.0	697.6	22.4	< 0.04	0.52	61.6	0.37
AT6	Las Pintas	250	7.2	33.6	718	6.21	102.0	33.9	31.2	16	14.5	435.2	5.9	0.03	0.32	40	0.04
AT7	Garabatos	200	6.8	25	188.9	6.73	16.1	1.2	2	0.4	2.2	24.4	9.7	4.53	0.01	22.8	0.03
AT8	Santa Ana Tepetitlan	250	6.9	25.8	240.4	6.02	38.5	2.3	5.8	1	30.6	18.3	34.6	71.6	0.01	45.3	0.02
AT9	Tapatíos 1	258	6.2	25	310	6.61	57.3	7.2	6.7	2.3	3.7	122.0	12.3	4.68	0.02	52.6	0.03
AT10	Topacio	235	6.7	21.8	569	6.34	63.8	21	14.3	6.3	5.2	242.2	8.9	0.42	0.1	38.4	0.03
AT11	Jardines del Bosque	250	7.1	27.8	309	5.75	26.5	3.5	7.8	2.6	14.0	30.5	29.4	5.76	0.03	29.8	0.02
AT12	Aqua Azul	40	7.1	29.1	354	3.3	44.1	8.9	23	7.4	50.3	24.4	95.2	11.8	0.12	41.4	0.02
AT13	Educadores Jalisc.	300	6.5	32.8	1111	3.93	14.6	6.3	16.8	4.8	1.3	102.5	1.1	0.43	0.12	35	0.02
AT14	Tanque Tepistán	292	7.1	32.5	325	4.22	23.3	6	5.1	2.6	4.8	58.6	7.1	1.12	0.04	22.9	0.02
AT15	Górgoros	80	7.4	30.6	231.7	6.5	38.4	4.5	4.2	1.3	11.0	78.1	25.2	5.40	0.02	48.6	0.03
AT16	Fray Pedro	70	7.3	30	334	4.28	21.0	6.5	4.6	2.2	5.6	68.3	8.5	1.43	0.03	20.1	0.02
AT17	Bajo La Arena B	80	8.7	24.6	218.5	4.32	20.8	2.8	1.8	0.5	0.7	53.7	2.2	2.40	0.01	48.3	0.04
AT18	S. Juan de Ocotán 1	120	7.9	22.5	345	4.95	27.1	8.5	4.5	4.2	2.0	87.8	1.5	0.05	0.02	25.6	0.04
AT19	Manantial Toliquilla	—	8.3	24.6	143.9	5.8	57.5	13.4	25	12.6	35.6	87.8	65.7	13.8	0.18	38.2	0.07
AT20	La Estancia 4	150	7.7	23.6	382	2.42	39.1	9.4	13.3	8.6	3.3	162.7	2.5	0.41	0.16	37.7	0.19
AT21	La Loma de S. Juan	60	7.5	25.3	569	4.4	38.3	8.6	16.7	12.9	7.2	172.2	6.1	0.95	0.18	44.3	0.03
AT22	Rancho Alegre	150	7.7	27.5	213.9	4.5	92.6	28.5	37.3	47.8	41.5	467.9	19.6	0.80	0.47	46.6	0.06
AT23	Mimbela	50	6.9	28.2	445	5.02	55.0	10.3	18.5	6.1	30.7	97.6	50.8	11.7	0.09	43.4	0.03
AT24	Tepistán 14	120	7.0	25.1	305	6.34	33.9	3.5	3.8	1.3	3.1	126.9	13.5	4.20	0.02	45.4	0.05
AT25	Fovisste	200	6.8	24.4	649	6.68	18.4	7.8	3.1	1.7	1.8	43.9	6.7	2.08	0.02	44.2	0.03
AT26	Power Center	90	7.5	32.6	190.7	5.65	35.3	6.1	7.5	2.7	2.1	113.7	8.6	1.58	0.04	41.9	0.05
AT27	Virreyes	300	6.8	29.4	363	4.81	43.9	7.2	5	3.2	1.1	146.4	1.5	0.73	0.02	51.6	0.12
AT28	Tepistán 61	275	6.7	24.6	222.4	5.94	27.0	4.4	4	1.6	1.4	83.0	3.5	2.07	0.02	47.8	0.35
AT29	Tepistán 56	270	6.9	33.7	298	7.66	16.7	1.7	7.1	2.1	7.6	30.5	21.0	6.75	0.01	19.1	0.02
AT30	Tepistán 70	250	7.1	26	107.8	4.83	20.0	8.8	7	1.9	2.9	60.8	12.3	5.72	0.07	47.5	0.03
AT31	Unid. Dep. Tonala	118	6.7	29.8	351	3.5	40.3	12.7	13.3	7.6	3.4	181.8	1.7	1.06	0.14	35.2	0.06
AT32	San Ismael	285	6.7	23.9	451	4.37	20.2	7.5	15.8	7.8	0.3	132.2	0.2	0.05	0.17	33.6	0.03
AT33	Tateposco 2	250	6.8	25.5	192.1	5.46	44.5	13.4	12.6	8	6.3	166.4	2.4	0.7	0.14	35.9	0.03
AT34	El Lindero	55	6.7	26.6	138.9	6.57	22.2	7.4	8.5	5.5	1.2	97.6	6.1	2.02	0.11	40.8	0.03
AT35	Vivero Los Amigos	24	6.6	27.3	234.7	7.72	19.9	16.6	10.1	4.1	2.7	53.7	40.1	25.4	0.08	30.9	0.02
AT36	El Taray	200	6.4	24.7	242	4.37	11.5	7.8	9.3	4.7	0.5	102.5	0.3	0.12	0.04	36	0.03
AT37	Viveros del Sur	54	6.3	27.7	160.3	5.63	14.1	0.6	1.9	0.3	2.1	29.3	2.1	1.19	0.01	20.3	0.14
AT38	Las Pomas	115	6.2	26.4	310	5.74	33.9	1.8	13.5	2.4	9.5	78.1	21.2	5.94	0.02	27.3	0.02
AT39	Potrero La Ordeña	64	6.7	25	165.9	5.93	31.9	8.8	13.2	8.2	10.1	97.6	23.4	17.7	0.15	25.5	0.03
AT40	Los Gigantes	62	8.0	31.6	182.8	5.65	30.9	2.7	4.7	1.3	2.8	58.6	6.9	4.87	0.02	38.3	0.02

Table 1. Continued.

ID	Well name	Well depth (m)	pH	T (°C)	EC (uS cm^{-1})	F	Zn	Li	Mn	Ba	^{3}H (TU)	^{2}H (‰)	^{18}O (‰)	Water type
AT1	Toluquilla 1	300	7.3	25	345	0.95	0.040	0.06	< 0.01	0.05	1.70	-64.3	-8.6	Na-Ca-HCO ₃
AT2	Toluquilla 6	300	7.0	25	1619	0.33	0.066	0.33	0.26	0.5	0.70	-68.4	-9.3	Mg-Na-HCO ₃
AT3	Toluquilla 17	200	7.0	25	2310	0.65	0.018	0.33	0.51	0.32	0.70	-66.5	-8.8	Mg-Na-HCO ₃
AT4	Toluquilla 22	300	7.0	31.8	1792	0.99	0.076	0.37	0.22	0.26	1.20	-67.4	-9.1	Mg-Na-HCO ₃
AT5	Toluquilla 7	230	7.0	36.4	1900	3.50	0.088	0.47	0.83	0.39	0.40	-66.5	-8.9	Mg-Na-HCO ₃ -Cl
AT6	Las Pintas	250	7.2	33.6	718	0.26	0.023	< 0.05	0.04	0.08	0.90	-64.7	-8.8	Na-HCO ₃
AT7	Garabatos	200	6.8	25	188.9	1.01	0.020	< 0.05	< 0.01	< 0.02	2.20	-70.5	-9.6	Na-HCO ₃ -SO ₄
AT8	Santa Ana Tepetitlan	250	6.9	25.8	240.4	3.79	0.005	0.08	< 0.01	< 0.02	0.60	-71.5	-9.9	Na-NO ₃ -Cl-SO ₄
AT9	Tapatíos 1	258	6.2	25	310	0.97	0.224	0.09	< 0.01	< 0.02	1.20	-71.1	-9.8	Na-HCO ₃
AT10	Topacio	235	6.7	21.8	569	0.84	0.092	< 0.05	< 0.01	0.05	0.90	-65.2	-8.9	Na-Ca-Mg-HCO ₃ -SO ₄ -Cl
AT11	Jardines del Bosque	250	7.1	27.8	309	0.46	0.046	< 0.05	< 0.01	0.04	2.10	-63.9	-8.4	Na-Mg-Ca-HCO ₃
AT12	Aqua Azul	40	7.1	29.1	354	0.20	0.005	< 0.05	< 0.01	< 0.02	2.40	-47.5	-5.7	Na-Mg-Ca-HCO ₃
AT13	Educadores Jalisc.	300	6.5	32.8	1111	0.21	0.161	< 0.05	< 0.01	< 0.02	0.50	-67.0	-9.1	Na-Mg-HCO ₃
AT14	Tanque Tesistán	292	7.1	32.5	325	0.72	0.092	< 0.05	< 0.01	< 0.02	1.00	-64.4	-8.8	Na-Ca-HCO ₃
AT15	Górgoros	80	7.4	30.6	231.7	0.81	0.198	< 0.05	< 0.01	< 0.02	1.50	-65.6	-9.0	Na-Ca-Mg-HCO ₃
AT16	Fray Pedro	70	7.3	30	334	0.34	0.095	< 0.05	< 0.01	< 0.02	0.30	-62.4	-8.7	Na-Mg-HCO ₃
AT17	Bajo La Arena B	80	8.7	24.6	218.5	1.40	0.584	< 0.05	< 0.01	< 0.02	0.90	-72.2	-9.9	Na-Mg-Ca-HCO ₃
AT18	S. Juan de Ocotán 1	120	7.9	22.5	345	2.49	0.132	< 0.05	< 0.01	< 0.02	0.70	-67.1	-9.4	Na-Ca-HCO ₃ -SO ₄
AT19	Manantial Toluquilla	–	8.3	24.6	143.9	0.57	0.308	< 0.05	< 0.01	0.13	2.00	-59.2	-7.9	Na-HCO ₃ -F
AT20	La Estancia 4	150	7.7	23.6	382	0.32	0.294	< 0.05	< 0.01	0.03	0.40	-67.0	-9.4	Na-Ca-HCO ₃
AT21	La Loma de S. Juan	60	7.5	25.3	569	0.46	0.963	< 0.05	< 0.01	< 0.02	0.80	-67.8	-9.5	Na-Mg-Ca-HCO ₃
AT22	Rancho Alegre	150	7.7	27.5	213.9	0.94	0.397	0.16	0.13	0.12	0.50	-66.3	-9.3	Na-HCO ₃
AT23	Mimbela	50	6.9	28.2	445	0.22	0.008	< 0.05	< 0.01	0.03	1.90	-59.6	-7.9	Na-HCO ₃
AT24	Tesistán 14	120	7.0	25.1	305	0.37	0.020	0.06	< 0.01	< 0.02	1.90	-68.8	-9.6	Na-Ca-SO ₄ -HCO ₃ -Cl
AT25	Fovisste	200	6.8	24.4	649	0.35	0.035	< 0.05	< 0.01	< 0.02	0.80	-69.2	-9.5	Na-Ca-SO ₄ -Cl
AT26	Power Center	90	7.5	32.6	190.7	0.24	0.033	< 0.05	< 0.01	< 0.02	1.60	-68.3	-9.5	Ca-Na-Mg-HCO ₃
AT27	Virreyes	300	6.8	29.4	363	1.16	0.113	0.06	< 0.01	< 0.02	0.80	-70.9	-10.0	Na-HCO ₃
AT28	Tesistán 61	275	6.7	24.6	222.4	0.39	0.431	< 0.05	< 0.01	< 0.02	1.60	-69.4	-9.7	Na-HCO ₃ -SO ₄
AT29	Tesistán 56	270	6.9	33.7	298	0.22	0.019	< 0.05	< 0.01	< 0.02	1.70	-66.5	-9.3	Na-HCO ₃
AT30	Tesistán 70	250	7.1	26	107.8	0.390	0.048	< 0.05	< 0.01	< 0.02	1.70	-67.8	-9.4	Na-HCO ₃
AT31	Unid. Dep. Tonala	118	6.7	29.8	351	0.26	0.112	< 0.05	< 0.01	< 0.02	0.70	-65.6	-9.0	Na-HCO ₃
AT32	San Ismael	285	6.7	23.9	451	0.06	0.100	< 0.05	< 0.01	0.03	0.70	-64.8	-8.8	Na-Ca-HCO ₃ -SO ₄ -Cl
AT33	Tateposco 2	250	6.8	25.5	192.1	0.34	0.130	< 0.05	< 0.01	< 0.02	0.70	-64.5	-8.9	Na-HCO ₃
AT34	El Lindero	55	6.7	26.6	138.9	0.18	0.182	< 0.05	< 0.01	0.03	2.00	-68.9	-9.6	Na-HCO ₃
AT35	Vivero Los Amigos	24	6.6	27.3	234.7	0.03	0.070	< 0.05	< 0.01	< 0.02	2.90	-64.5	-9.4	Na-HCO ₃
AT36	El Taray	200	6.4	24.7	242	0.26	0.341	< 0.05	< 0.01	< 0.02	0.70	-67.1	-9.3	Na-HCO ₃
AT37	Viveros del Sur	54	6.3	27.7	160.3	4.90	0.084	< 0.05	0.02	< 0.02	0.50	-71.6	-10.3	Na-HCO ₃
AT38	Las Pomás	115	6.2	26.4	310	1.67	1.040	0.08	< 0.01	< 0.02	1.80	-68.5	-9.5	Na-Ca-HCO ₃ -SO ₄
AT39	Potrero La Ordeña	64	6.7	25	165.9	1.25	0.065	< 0.05	< 0.01	< 0.02	1.00	-68.3	-9.4	Na-Ca-HCO ₃
AT40	Los Gigantes	62	8.0	31.6	182.8	1.71	0.252	0.06	< 0.01	< 0.02	0.50	-70.4	-9.6	Na-Ca-Mg-HCO ₃

Groundwater flow processes and mixing in active volcanic systems

A. Hernández-Antonio et al.

- [Title Page](#)
- [Abstract](#)
- [Conclusions](#)
- [Tables](#)
- [Back](#)
- [Full Screen / Esc](#)
- [Printer-friendly Version](#)
- [Interactive Discussion](#)

Table 2. Median values of water chemistry of the groundwater subgroups determined from HCA. Data are given in mg L^{-1} , except for pH (standard units), EC (electrical conductivity in $\mu\text{S cm}^{-1}$), temperature ($^{\circ}\text{C}$), ^3H (in UT), $\delta^2\text{H}$ (in ‰ VSMOW) and $\delta^{18}\text{O}$ (in ‰ VSMOW). Note: DO = dissolved oxygen.

Group	N	Parameter	pH	T	EC	SDT	DO	^3H	$\delta^2\text{H}$ (‰)	$\delta^{18}\text{O}$	HCO_3	K	Mg	Si	Ca	Fe	Na	Sr	Zn	F	Cl
1	6	Average	6.9	33.8	1575	733	5.4	0.73	-66.65	-9.02	852.7	41.0	79.5	45.9	54.4	0.14	130.3	0.46	0.11	1.11	87.2
		Median	7.0	33.6	1706	710	5.4	0.70	-66.52	-8.98	864.5	38.5	98.0	43.3	48.0	0.10	130.5	0.46	0.07	0.80	76.3
2	12	Average	7.2	30.2	300	95	4.5	0.66	-66.09	-9.10	128.0	9.2	5.9	33.6	10.9	0.04	31.2	0.10	0.23	0.67	3.5
		Median	7.1	29.9	317	89	4.4	0.70	-66.27	-9.07	117.4	8.2	5.6	35.6	13.0	0.03	29.0	0.11	0.13	0.34	3.3
3	3	Average	6.8	23.4	556	229	4.7	2.1	-55.5	-7.2	69.9	10.9	8.7	41.0	22.2	0.04	52.2	0.13	0.11	0.3	38.9
		Median	6.7	23.9	569	241	5.0	2.0	-59.2	-7.9	87.8	10.3	7.4	41.4	23.0	0.03	55.0	0.12	0.01	0.2	35.6
4	19	Average	7.0	25.3	254	84	6.0	1.5	-68.5	-9.5	75.5	5.4	2.5	38.6	6.6	0.06	29.4	0.04	0.17	1.1	6.2
		Median	6.8	25.0	235	77	5.9	1.6	-68.8	-9.5	78.1	4.5	2.1	44.0	6.7	0.03	27.0	0.02	0.07	0.8	2.9

- [Title Page](#)
- [Abstract](#) [Introduction](#)
- [Conclusions](#) [References](#)
- [Tables](#) [Figures](#)
- [◀](#) [▶](#)
- [◀](#) [▶](#)
- [Back](#) [Close](#)
- [Full Screen / Esc](#)
- [Printer-friendly Version](#)
- [Interactive Discussion](#)

Table 2. Continued.

Group	N	Parameter	pH	T	EC	SDT	NO ₃ -N	SO ₄	Li	Ba	Mn
1	6	Average	6.9	33.8	1575	733	0.17	11.0	0.29	0.28	0.33
		Median	7.0	33.6	1706	710	0.05	6.5	0.33	0.29	0.24
2	12	Average	7.2	30.2	300	95	0.97	3.9	0.01	0.04	0.01
		Median	7.1	29.9	317	89	0.57	2.4	0.00	0.03	0.01
3	3	Average	6.8	23.4	556	229	12.4	70.6	0.00	0.08	0.01
		Median	6.7	23.9	569	241	11.8	65.7	0.00	0.08	0.01
4	19	Average	7.0	25.3	254	84	9.1	15.5	0.02	0.04	0.01
		Median	6.8	25.0	235	77	4.5	12.3	0.00	0.04	0.01

Table 3. Rotated component matrix of the factor analysis for groundwater samples from the Atemajac Toluquilla aquifer system. Coefficients between –0.1 and 0.1 are suppressed. Note: DO = dissolved oxygen, T = temperature, EC = electrical conductivity.

Variable	PC1	PC2	PC3	PC4
pH				0.47
T	0.24	0.23	0.29	
EC	0.32			
DO		–0.25		
³ H		–0.37		0.15
² H			0.45	–0.20
¹⁸ O			0.45	
HCO ₃	0.32			
K	0.32			
Mg	0.33			
SiO ₂			–0.23	
Ca	0.32			
Fe			–0.37	
Na	0.33			
Sr	0.32		0.13	
Zn				
F			–0.371	
Cl	0.3			
NO ₃		–0.40		
SO ₄		–0.50		
Eigenvalue	8.43	3.38	2.21	1.34
% of variance	42	17	11	7
Cum. % variance	42	59	70	77

Groundwater flow processes and mixing in active volcanic systems

A. Hernández-Antonio et al.

[Title Page](#)

[Abstract](#)

[Introduction](#)

[Conclusions](#)

[References](#)

[Tables](#)

[Figures](#)

◀

▶

◀

▶

[Back](#)

[Close](#)

[Full Screen / Esc](#)

[Printer-friendly Version](#)

[Interactive Discussion](#)

Table 4. Mixing proportions from The multivariate mixing and mass-balance model, M3, using the following reference waters: no. 5 as a reference for hydrothermal fluids; no. 12 as a reference for polluted water; and no. 37 as reference for groundwater.

Well ID	Well group	% hydrothermal water	% fresh groundwater	% polluted water
2	1	77	23	0
3	1	75	21	4
4	1	87	10	3
5	1	100	0	0
6	1	32	50	18
22	1	45	42	13
10	2	13	63	24
13	2	8	76	16
14	2	2	70	28
16	2	4	71	25
18	2	5	80	15
20	2	11	72	17
21	2	13	70	17
31	2	12	69	19
32	2	8	69	23
33	2	11	67	22
36	2	5	80	15
40	2	3	85	12
12	3	0	0	100
19	3	9	28	63
23	3	4	37	59
1	4	4	59	37
7	4	–	–	–
8	4	2	75	23
9	4	5	75	20
11	4	–	–	–
15	4	0	64	36
17	4	2	87	11
24	4	0	72	28
25	4	1	79	20
26	4	3	72	25
27	4	6	81	13
28	4	1	77	22
29	4	–	–	–
30	4	1	70	29
34	4	1	76	23
35	4	–	–	–
37	4	0	100	0
38	4	0	72	28
39	4	6	69	25

Groundwater flow processes and mixing in active volcanic systems

A. Hernández-Antonio et al.

[Title Page](#)

[Abstract](#)

[Introduction](#)

[Conclusions](#)

[References](#)

[Tables](#)

[Figures](#)

◀

▶

◀

▶

[Back](#)

[Close](#)

[Full Screen / Esc](#)

[Printer-friendly Version](#)

[Interactive Discussion](#)

Groundwater flow processes and mixing in active volcanic systems

A. Hernández-Antonio et
al.

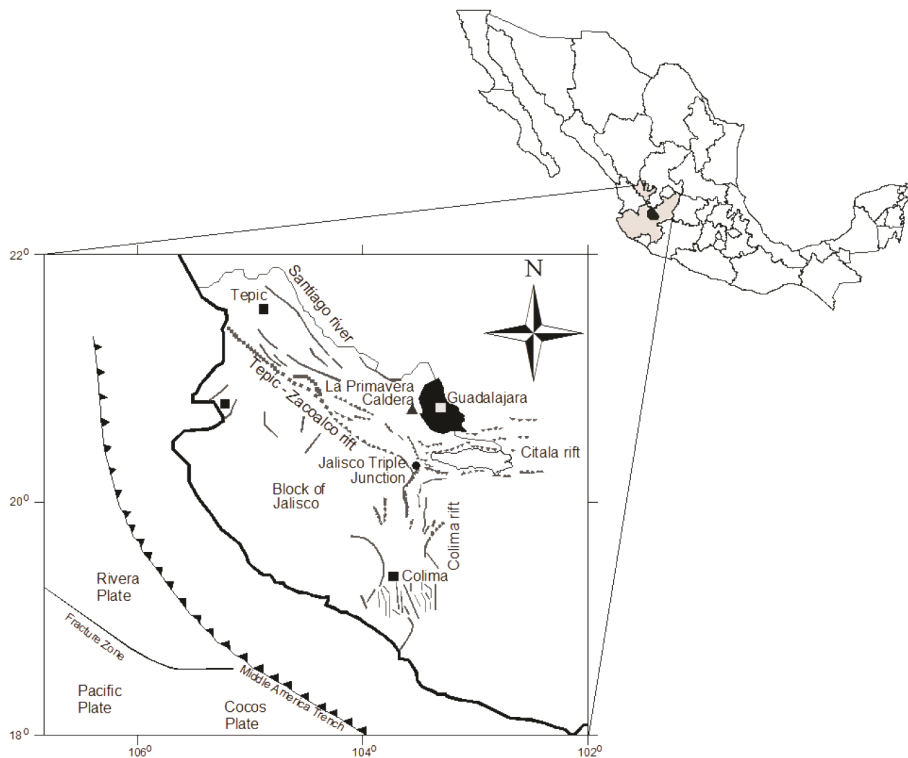


Figure 1. Location of study area (black area) in Mexico and tectonic structures of western Central Mexico.

1624

A small rectangular icon with a black border. Inside, on the left, is a white circle with the letters 'cc'. To its right is another white circle containing a black silhouette of a person. Below these symbols, the letters 'BY' are printed in a small, black, sans-serif font.

Groundwater flow processes and mixing in active volcanic systems

A. Hernández-Antonio et
al.

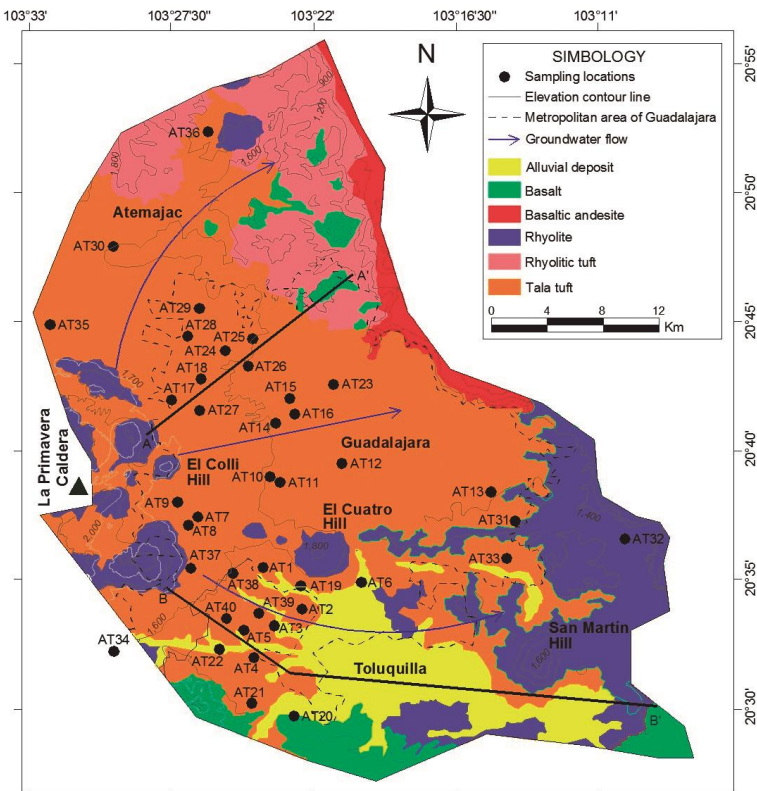


Figure 2. Geologic map of the Atemajac–Toluquilla study unit with groundwater flow direction and locations of sampled wells.

Title Page

Abstract

Introduction

Conclusion:

References

Tables

Figures

1

▶

Back

Close

Full Screen / Esc

[Printer-friendly Version](#)

Interactive Discussion

Groundwater flow processes and mixing in active volcanic systems

A. Hernández-Antonio et al.

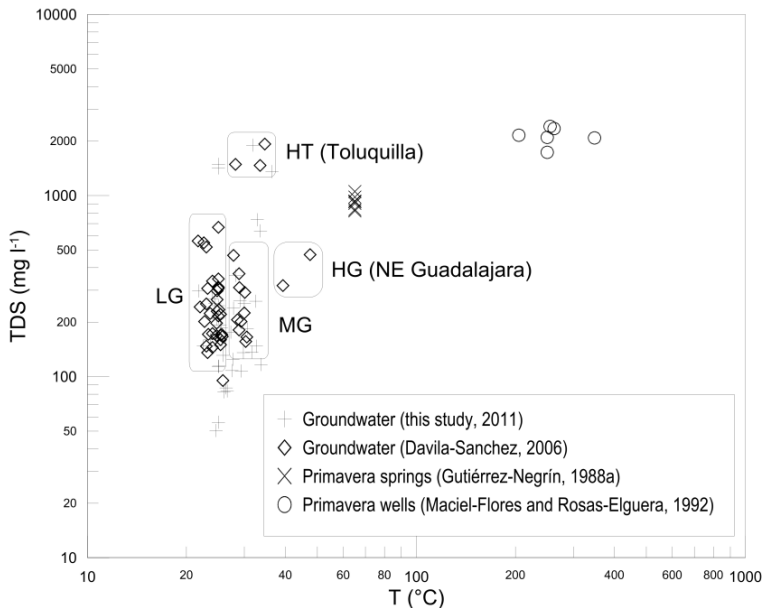


Figure 3. Plot of water temperature vs. total dissolved solids for different groundwater collecting campaigns in the study area. The delimitation of classified wells according to Sánchez-Díaz (2007) is also shown. Note: HT = hydrothermal water from Toluquilla, HG = hydrothermal water from springs NE of Guadalajara, LG = local groundwater, MG = mixed groundwater (HT and LG).

Groundwater flow processes and mixing in active volcanic systems

A. Hernández-Antonio et
al.

Title Page

Abstract

Introduction

Conclusion

References

Tables

Figures

1

1

Back

Close

Full Screen / Esc

Interactive Discussion

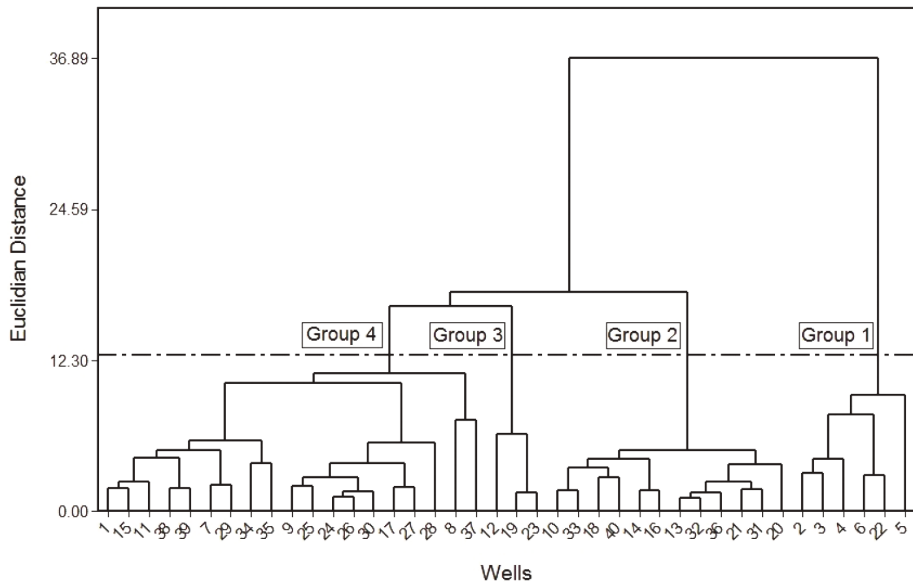


Figure 4. Dendrogram showing HCA classification with groups and subgroups of samples of the Atemajac–Toluquilla aquifer system. The dashed line indicates the “phenon line”, an arbitrary line that defines subgroups.

Groundwater flow processes and mixing in active volcanic systems

A. Hernández-Antonio et
al.

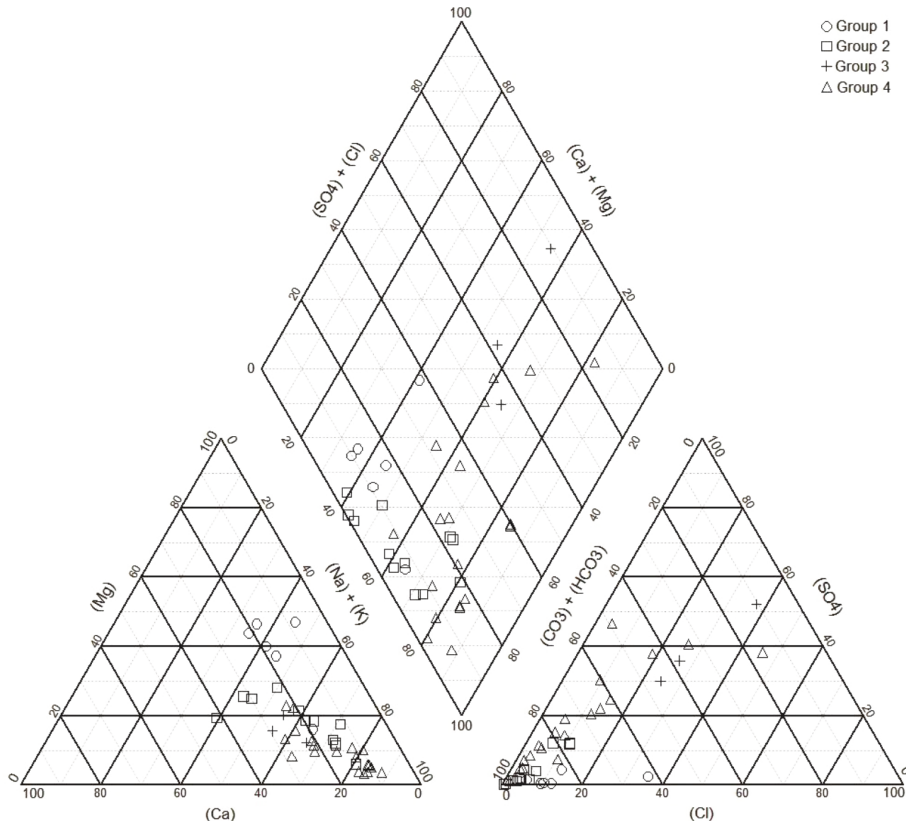


Figure 5. Piper diagram of groundwater samples from the Atemajac–Toluquilla aquifer system with well groups.

Groundwater flow processes and mixing in active volcanic systems

A. Hernández-Antonio et
al.

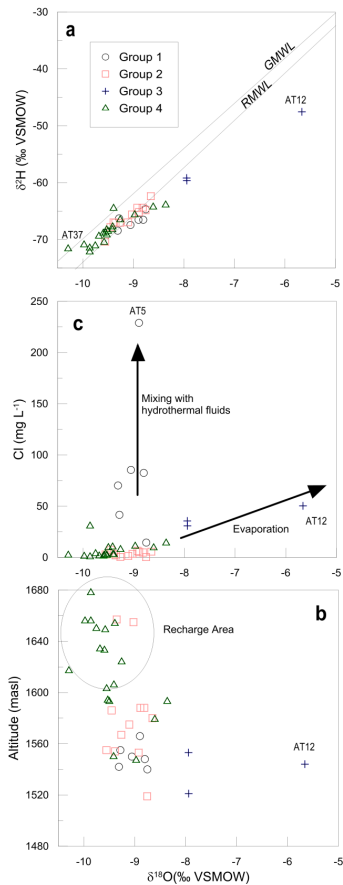


Figure 6. (a) Deuterium and oxygen-18 in groundwater from the ATAS, the Global Meteoric Water Line (GMWL) (Rozanski et al., 1993) and the Regional Meteoric Water Line (RMWL) (Wassenaar et al., 2009); (b) oxygen-18 vs. chloride concentration; and (c) oxygen-18 vs. altitude.

Groundwater flow processes and mixing in active volcanic systems

A. Hernández-Antonio et al.

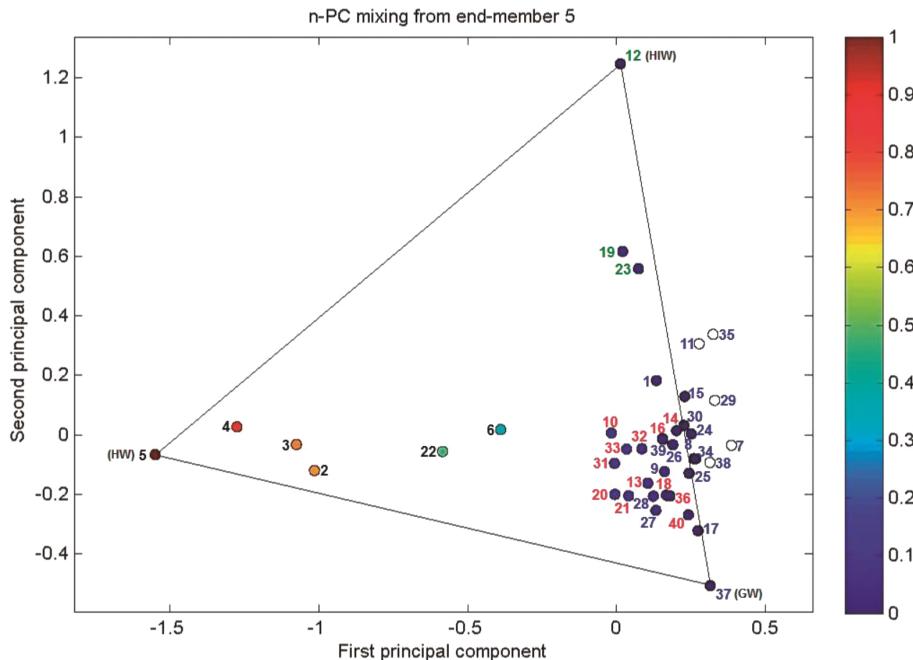


Figure 7. PC plot of the M3 model from mixing of hydrothermal fluids, cold groundwater and polluted waters. Note: Numbers with black font represent group 1, with red font group 2, with green font group 3, and with blue font group 4.

Groundwater flow processes and mixing in active volcanic systems

A. Hernández-Antonio et al.

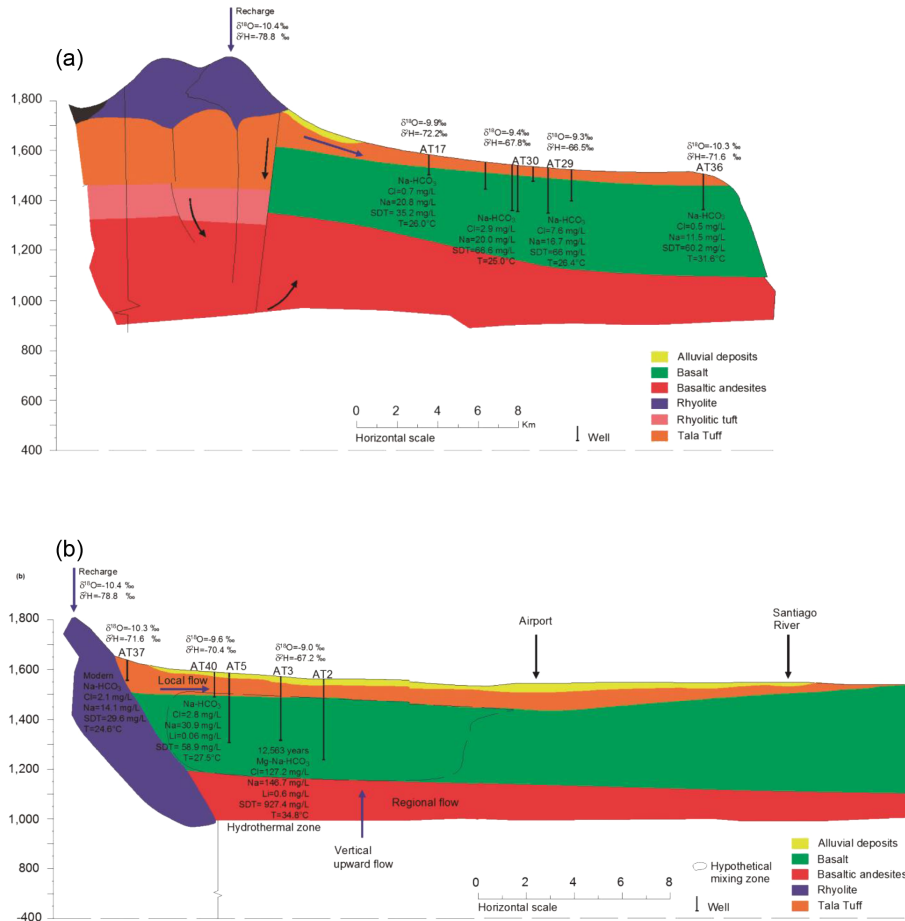


Figure 8. Schematic vertical flow sections of the Atemajac–Toluquilla aquifer unit: **(a)** Atemajac Valley A-A, **(b)** Toluquilla Valley B-B. The geographical location of the sections is shown in Fig. 1.